Adsorption of Neutral Polymers: Interpretation of the Numerical Self-Consistent Field Results

A. Johner,[†] J. Bonet-Avalos,[▽] C. C. van der Linden,[‡] A. N. Semenov,[†,§] and J. F. Joanny*,[†]

Institut Charles Sadron, CNRS-ULP, 67083 Strasbourg Cedex, France, Departement of Physical and Colloid Chemistry, Wageningen Agricultural University, Dreijenplein 6, 6703 HB Wageningen, The Netherlands, Polymer Laboratory, University of Moscow, Moscow, Russia, and Departement de Fisica Fondamental, Facultat de Fisica, Universitat de Barcelona, Barcelona, Spain

Received October 31, 1995; Revised Manuscript Received February 9, 1996[⊗]

ABSTRACT: We use results on polymer absorption obtained from a recent mean-field theory with two order parameters to interpret numerical results of the Scheutjens and Fleer approach. An extension of the analytical theory accounting for the local swelling of the polymer is also presented and discussed.

I. Introduction

When a polymer solution is brought into contact with an adsorbing wall, the monomer concentration rises at the wall and relaxes toward its bulk value over a distance of the order of one bulk correlation length ξ. The adsorbed polymer usually remains attached to the wall after cautious rinsing of the bulk solution.[1] Polymer adsorption is widely used in technological applications such as adhesion, lubrication, stabilization, or controlled flocculation of colloidal dispersions.[2] Adsorption on natural or biocompatible substrates also plays an important role in medicine.

The adsorbed polymer layer can be described in terms of loop and tail size distributions.[3] In some of the applications it probably is sufficient to cover the surface with a soft polymer layer whatever its detailed structure; this is true to some extent for colloidal stabilization. On the other hand, polymer loops dangling from the surface into the solution may entangle with free chains, and the coupling between the bulk and the interface is certainly sensitive to the loop size distribution.[4] In a similar way loops and tails do not penetrate equally well into a rubber; the relative size of loops and tails should be important in the adhesion between a solid and a rubber mediated by a polymer layer.[5] The details of the layer structure also certainly matter in biological applications when recognition processes are involved.

Global measurements on adsorbed polymer layers such as the determination of the adsorbance Γ (total amount of polymer linked to the surface) or of some moment of the concentration profile (by means of scattering techniques, flow experiments, or optical experiments) are now standard though not always easy. Very recently more detailed information on the shape of the concentration profile (by neutron scattering or neutron reflectivity experiments) and on the bound monomer fraction (by NMR and IR spectroscopy experiments) has been obtained. There is also some evidence of the loop structure from AFM investigations.[6,7] A review of the experimental work is found in a recent monograph by the Dutch group.[3]

Since the seminal work of Silberberg,[8] many theoretical papers have been devoted to polymer adsorption. At the mean-field level, numerical methods have been worked out by the Dutch group for various polymeric systems.[9,10,3] They have obtained detailed concentration profiles for the loop and tail contributions.[3] The external part of the layer is mostly built up by the tails, whereas close to the wall the monomers mainly belong to loops. Analytical mean-field calculations have been essentially performed in the so-called ground state dominance approximation. A more detailed calculation has been proposed recently that distinguishes between loops and tails and covers the entire concentration range from dilute to concentrated solutions.[11]

For neutral flexible polymers adsorbed onto a solid wall, a theory has been constructed beyond the mean-field level;[12] this theory is based on the analogy between the partition function of a self-avoiding chain and the correlation function of a magnet in the zero component limit, first recognized by de Gennes.[13] This analogy links the physics of infinitely long chains to critical phenomena and gives a basis to the so-called scaling analysis that successfully predicts the main qualitative features of polymer adsorption.[14] A scaling argument due to de Gennes shows that the overall concentration profile falls off the wall as $c(z) \simeq z^{-4/3}$, in contrast to the mean-field prediction $c(z) \simeq z^{-2}$. More precisely, one distinguishes the proximal region closest to the wall, of thickness $D \simeq \delta^{-1}$, where δ is the adsorption strength, the central region where the power law profile is expected over about one correlation length ξ (in the dilute regime ξ merges with the swollen radius R), and the distal region where the concentration relaxes exponentially toward its bulk value. The loop size distribution inside the polymer layer (central region) has been predicted first by de Gennes, assuming that the concentration is mainly due to loops, as $D(n) \simeq n^{-11/5}$.

Recently, it was argued that, in the dilute regime, this approach only applies in the very vicinity of the adsorbing wall,[15,11] tails being dominant beyond a distance $z^* \simeq N^{1/(d-1)}$; here d is the space dimension. The intermediate length scale z^* is the only length scale in the central regime where the concentration can be written in a self-similar form, $c(z) \simeq z^{*-4/3} f(z/z^*)$. The $z^{-4/3}$ power law is only valid asymptotically on either side of z^*. The mean-field calculation suggests that the amplitude A (in $c(z) = Az^{-4/3}$) at large distances ($z > z^*$) is larger than that at small distances ($z < z^*$) by a factor of order 10

[†] Institut Charles Sadron.
[‡] Wageningen Agricultural University.
[§] University of Moscow.
[▽] Universitat de Barcelona.
[⊗] Abstract published in *Advance ACS Abstracts,* April 1, 1996.

S0024-9297(95)01637-8 CCC: $12.00

and that the region $z \simeq z^*$ where neither of the assymptotics is accurate is broad.[11]

Scaling theories have also been proposed for more concentrated solutions. Marques and Joanny have proposed a qualitative picture with two characteristic concentrations[16] above the overlap concentration: $\phi_1 \simeq N^{-2/3}$, where the polymer chains start to build up large loops dangling out of the adsorption layer, and $\phi_2 \simeq N^{-4/7}$, where the adsorbance starts to be dominated by the large loops and tails.

Subsequently Daoud and Jannink[17] proposed that the adsorbed layer thickness is not the radius of gyration but a new length, $\lambda \simeq N\phi^{3/4}$, that crosses over smoothly from the bulk correlation length ξ at ϕ_1 to the radius of gyration of the chains in the semidilute solution R at ϕ_2 as the concentration is increased. We recently showed[11] that this length rather corresponds to the crossover length z^*. At the same time, Guiselin[18] worked out more details of the concentration profile and tried to distinguish between loops and tails using a free energy based on an approximate mixing entropy of the loops. This kind of theory in general approximates the susceptibility exponent γ in a rather uncontrolled way. An example is given below.

The mean-field theory is not expected to give the correct qualitative picture in the sense that it becomes increasingly bad when the length of the swollen chain diverges. Nevertheless, mean field is accurate under so-called marginal solvency conditions where the excluded volume is weak, $vN^{1/2} < 1$, a situation that is not unusual in experiments. Besides, a mean-field theory is well suited for concentrated solutions where the adsorbance is dominated by the large loops and tails outside the adsorption layer; these loops follow overall Gaussian statistics, and one merely has to correct for the local swelling at the scale of the bulk correlation length. The adsorption from such concentrated solutions has often been used recently as a first step to obtain a so-called pseudobrush by subsequent dilution.[19]

From a more formal point of view, mean field becomes qualitatively correct in four dimensions, where the excluded volume interaction is only marginally relevant. We thus expect that most of the important features of the adsorption profile have a mean-field analog (this is not always true: the rather subtle proximal effect pointed out by Eisenriegler, Binder, and Kremer[20] has no mean-field equivalent). Mean-field calculations contain the length scales of interest, agree with the scaling predictions formulated for four dimensions, and give some indication on how fast these (asymptotic) laws are approached.

The analytical and numerical mean-field approaches are complementary. The analytical approach is more comprehensive in the sense that it gives simple asymptotic laws for most of the parameters of interest; it also gives some insight into the physical mechanisms involved. The numerical approach allows the incorporation of more details of the free energy and is thus more accurate for polymers of finite molecular weight. The main aim of this paper is to explicitly compare recent analytical mean-field results to numerical mean-field results, in order to unify as much as possible the descriptions developed by our two groups (and others).

We first recall the main analytical results obtained recently[11] and the physical content of the so-called Scheutjens and Fleer numerical approach (section II). The analytical results are then used to interpret the numerical mean-field results from the Dutch group (section III). We finally propose an extension of the analytical mean-field theory to the self-avoiding chain limit.

II. Mean-Field Theory

1. Two-Order Parameter Theory. An analytical mean-field theory has been recently proposed[11] that accounts for both loop and tail monomers of adsorbed and free chains. The full theory is restricted to distances from the wall smaller than the free chain radius. Here we give a simplified version of the theory that does not consider the free chains. This simplified theory is valid at distances from the wall smaller than the adsorbed layer thickness λ, where the free chain concentration can be neglected.

In contrast to the standard ground state dominance approximation, two order parameters, $\varphi(z)$ and $\psi(z)$, are introduced. The former, $\varphi(z)$, is related to the partition function of a nonadsorbed chain, whereas the latter, $\psi(z)$, is related to the partition function of an adsorbed chain. We represent the monomer/wall interaction by a localized Dirac δ potential; the eigenstate expansion of the partition functions then involves one bound state and a continuum of free states.

The partition function of an adsorbed chain is dominated by the bound state of energy $-\epsilon$ provided $\epsilon N \gg 1$. The order parameter ψ is related to the partition function of an adsorbed chain with one end at position z via:

$$Z_a(z) = \exp(\epsilon N)\psi(z)\int_0^\infty \psi(z')\,dz'$$

(as in the standard ground state approximation).

The order parameter φ is the Laplace transform of the partition function of a free chain $Z_{free}(z,n)$ with respect to chain length:

$$\varphi(z) = \int_0^\infty Z_{free}(z,n)\exp(-\epsilon n)\,dn$$

It is defined so that the statistical weight of all the adsorbed configurations with a tail monomer located at z: $\int_0^N Z_a(N-n,z)Z_{free}(z,n)\,dn$ is proportional to the product $\psi\varphi$. The order parameter φ describes a tail section dangling beyond z.

The order parameters are normalized so that the concentration of loop monomers $c_l(z)$ is $c_l(z) = \psi(z)^2$, that of tail monomers is then $c_t(z) = B\psi(z)\varphi(z)$, and the end point density of adsorbed chains is $c_e(z) = B\psi(z)$. The normalization constant B is obtained from the conservation of the end points. For moderately concentrated solutions (with bulk concentration $\phi_0 < \phi_2$), the adsorbance Γ is dominated by the small loops (and is essentially independent of chain length); this fixes B from

$$B\int_0^\infty \psi(z')\,dz' = 2\Gamma/N \qquad \text{(II.1)}$$

The energy ϵ of the bound state is fixed by balancing the chemical potentials of adsorbed and free chains. When the absorbance is dominated by the (short) loops:

$$\epsilon = \frac{1}{N}\log\frac{\Gamma^2}{\phi_0\left(\int_0^\infty \psi(z')\,dz'\right)^2} \qquad \text{(II.2)}$$

The equations governing the order parameters φ and ψ are derived from Edwards[21] Schroedinger-like equation for the partition functions of adsorbed and free chains:

$$0 = -\frac{a^2}{6}\frac{d^2\psi}{dz^2} + (U(z)+\epsilon)\psi(z) \qquad \text{(II.3)}$$

$$1 = -\frac{a^2}{6}\frac{d^2\varphi}{dz^2} + (U(z)+\epsilon)\varphi(z)$$

where the molecular potential is linear in the local concentration $U(z) = \psi\psi + B\varphi\psi - \phi_0$, the excluded volume parameter

being taken as unity. The order parameter equations are supplemented by the boundary conditions:

$$\frac{1}{\psi}\frac{d\psi}{dz}\Big|_w = -\frac{1}{D}$$

$$\varphi|_w = 0 \qquad \text{(II.4)}$$

$$\lim_{z\to\infty} \psi(z) = 0$$

where the adsorption length D is imposed by the adsorption strength. The solution of these equations is briefly discussed in section III. We next describe the numerical mean-field calculation performed by Van der Linden et al. using the Scheutjens and Fleer method.

2. Numerical Mean-Field Theory. The theory of Scheutjens and Fleer is a lattice theory: Each polymer segment or solvent molecule is assumed to occupy exactly one lattice site. We use a simple cubic lattice, in which each lattice site has six neighbors. The lattice constant a is chosen to be unity for simplicity. Upon adsorption, a volume fraction profile $\{\phi(z)\}$ develops perpendicular to the surface. All inhomogeneities parallel to the surface are neglected. The surface is located at $z = 0$, adsorption takes place at $z = 1$, the layer adjacent to the surface, and the bulk solution is far away from the surface at $z = M$, where M is a large number. The dimensionless potential energy $U(z)$ that a polymer segment in an athermal solvent feels in layer z is written as

$$U(z) = -\chi_s\delta_{1z} + U'(z) \qquad \text{(II.5)}$$

Here, $U'(z)$ is the "space-filling potential", essentially a Lagrange multiplier ensuring that the lattice is completely filled. The Silberberg adsorption energy parameter for the polymer/solvent pair on the surface is χ_s; the Kronecker δ_{1z} ensures that the adsorption energy is only felt by segments on the surface.

The solvent molecules occupy exactly one lattice site and are distributed in the system according to Boltzmann's law:

$$\phi_s(z) = \phi_{s,0}e^{-U'(z)} \qquad \text{(II.6)}$$

where $\phi_{s,0} = 1 - \phi_0$ is the solvent bulk volume fraction. The exponential factor in eq II.6 is called the free segment-weighting factor $G(z)$:

$$G(z) = e^{-U(z)} \qquad \text{(II.7)}$$

In placing polymers on a lattice, we have to keep in mind that the segments are connected. If segment number s is in layer z, segment $s + 1$ has to be either in layer $z - 1$, layer z, or layer $z + 1$. The statistical weight of a segment number s of the polymer to be in layer z, given that the first segment is free to distribute analogously to eq II.6, is called the end segment distribution function (edf) $G(z,s|1)$. Analogously, we can define the edf starting from the other end N, $G(z,s|N)$. The edf of segment s can be obtained from the edf of the preceding one according to a recurrence relation:

$$G(z,s|1) = G(z)\frac{G(z-1,s-1|1) + 4G(z,s-1|1) + G(z+1,s-1|1)}{6}$$

$$G(z,s|N) = G(z)\frac{G(z-1,s+1|N) + 4G(z,s+1|N) + G(z+1,s+1|N)}{6} \qquad \text{(II.8)}$$

The end points do not have a preceding segment, so their edf's are simply equal to the corresponding free segment weighting factor: $G(z,N|N) = G(z,1|1) = G(z)$. Combining the two ends and summing over all segments, we arrive at the volume fraction profile of the polymer:

$$\phi(z) = \frac{\phi_0}{N}\sum_s \frac{G(z,s|1)G(z,s|N)}{G(z)} \qquad \text{(II.9)}$$

The division by $G(z)$ is necessary to correct for the double counting of segment s, and ϕ_0/N is the proper normalization. Equation II.9 is known as the composition law: It relates the volume fraction profile $\{\phi(z)\}$ to the potential profile $\{U(z)\}$. Equation II.6 relates the potential profile to the volume fraction profile. The set of coupled equations is solved numerically under the constraint that the sum of the volume fractions of polymer and solvent equals one, *i.e.*, the lattice is completely filled. The result is the self-consistent solution.

III. Explicit Mean-Field Solutions

1. Dilute Regime. When the bulk solution is dilute, the bulk concentration ϕ_0 can be neglected in the molecular potential U. Three regions can then be distinguished in the layer: (i) the proximal region closest to the wall within a distance D, comparable to the monomer size in the limit of strong adsorption, (ii) the central region in the intermediate range ($D < z < \lambda = \epsilon^{-1/2}$) where the concentration is high and thus U dominates over ϵ, and (iii) the distal region ($z > \lambda$) where ϵ dominates over U.

The order parameter equations can be written in a dimensionless form as

$$0 = -\frac{d^2\tilde{\psi}}{d\zeta^2} + (\tilde{U} + \tilde{\epsilon})\tilde{\psi}$$

$$1 = -\frac{d^2\tilde{\varphi}}{d\zeta^2} + (\tilde{U} + \tilde{\epsilon})\tilde{\varphi} \qquad \text{(III.1)}$$

with $\tilde{U} = \tilde{\psi}\tilde{\psi} + \tilde{\varphi}\tilde{\psi}$. The natural unit length is

$$l = \frac{a}{\sqrt{6}}\left(\frac{1}{B}\right)^{1/3} \qquad \text{(III.2)}$$

and the reduced variables are defined as

$$\zeta = z/l,\ \tilde{\psi}(\zeta) = \frac{\sqrt{6l}}{a}\psi(z),\ \tilde{\varphi}(\zeta) = \left(\frac{\sqrt{6l}}{a}\right)^{-2}\varphi(z),$$

$$\tilde{U}(\zeta) = \left(\frac{\sqrt{6l}}{a}\right)^{2}U(z),\ \tilde{\epsilon} = \left(\frac{\sqrt{6l}}{a}\right)^{2}\epsilon \qquad \text{(III.3)}$$

In the central region ϵ is negligible compared to U. Closer to the wall ($z \ll l$) the loop contribution dominates over the tail contribution, and we find the following asymptotic behavior:

$$\psi = \frac{a}{\sqrt{3}z}$$

$$\varphi = \frac{2}{a^2}z^2\log\left(\frac{l}{z}\right) \qquad \text{(III.4)}$$

$$U(z) = \frac{a^2}{3z^2}$$

Further away from the wall ($z \gg l$), the tail contribution

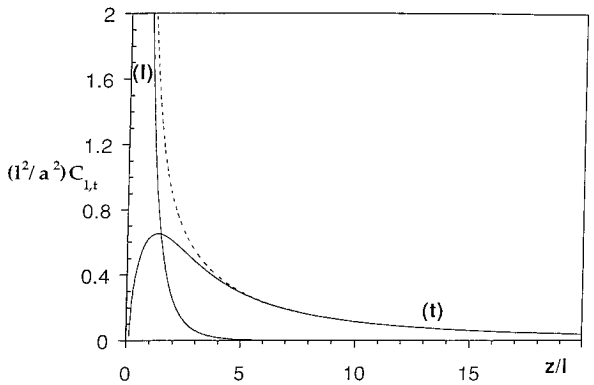

Figure 1. Crossover behavior around z^*. The reduced loop (l) and tail (t) concentrations (see text) are plotted against z/l. The loop concentration decays monotonically from the wall.

dominates over the loop contribution, and inside the central regime ($\lambda > z \gg l$):

$$\psi = \frac{10a^4}{Bz^4}$$

$$\varphi = \frac{1}{3a^2}z^2 \qquad \text{(III.5)}$$

$$U(z) = \frac{10a^2}{3z^2}$$

The large crossover between the two asymptotic behaviors has been obtained by numerical solution of eq III.1 and is shown in Figure 1. The concentrations of monomers belonging to loops and tails cross at a distance $z^* = 1.43l$ from the wall, whereas the loop contribution reaches its maximum at $z = 1.29l$.

The asymptotic analysis allows for the calculation of B and ϵ. From eqs II.1 and II.2 we obtain with a logarithmic accuracy:

$$l = \frac{a}{\sqrt{6}}\frac{1}{3^{1/3}2^{1/2}}\left(\frac{ND\sqrt{6}}{a}\right)^{1/3}\left(\log\left(\frac{Na^2}{D^2}\right)\right)^{1/3}$$

$$\epsilon = \frac{1}{N}\log\left(\frac{a^2}{\phi_0 D^2}\right) \qquad \text{(III.6)}$$

In the distal regime, the tail contribution still dominates, but the potential U is negligible compared to ϵ. In this regime the natural unit length is

$$\lambda = \frac{a}{\sqrt{6}}\epsilon^{-1/2} \qquad \text{(III.7)}$$

and the concentration of adsorbed polymer decays exponentially:

$$\psi \simeq \frac{1}{B}\epsilon^2 \exp -(z/\lambda)$$

$$\varphi = \frac{1}{\epsilon} \qquad \text{(III.8)}$$

$$c_t \simeq \epsilon \exp -(z/\lambda)$$

$$c_l \simeq \frac{1}{B^2}\epsilon^4 \exp -(2z/\lambda)$$

In the crossover region between the central and the distal regime ($z \gg l$), the loop contribution to the

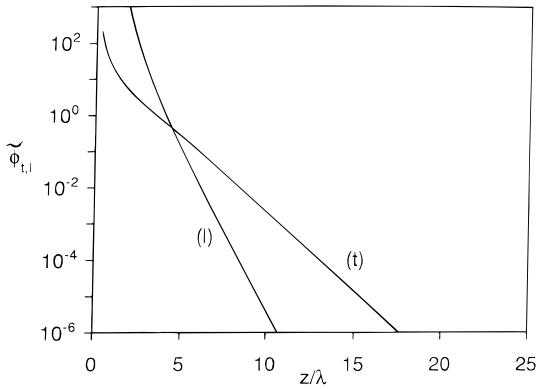

Figure 2. Crossover behavior around λ. The reduced loop contribution (l), $\tilde{\phi}_l = B^2\lambda^8 C_l$, and tail contribution (t), $\tilde{\phi}_t$ $B^2\lambda^2 C_t$, are plotted against z/λ.

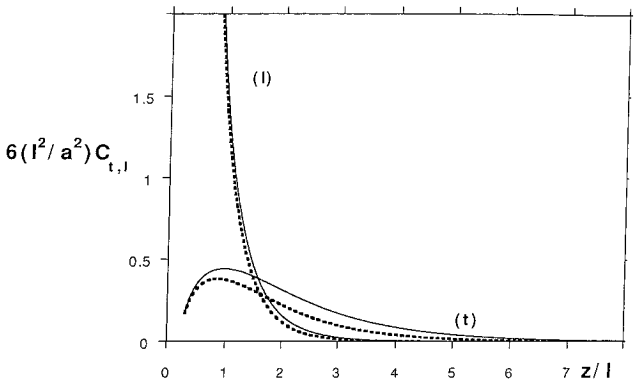

Figure 3. Reduced loop and tail contributions (see text) for finite $\tilde{\epsilon}$: $\tilde{\epsilon} = 0.64$ and 1 (dashed line).

molecular potential U is negligible. Choosing λ as a unit length rather than l, the concentration of loops and tails follows a universal master curve in the crossover region plotted in Figure 2.

At distances from the wall larger than λ, the free chains cannot be neglected. (We do not want to discuss free chain penetration in details here.) As shown elsewhere,[11] a weak minimum in the total concentration is expected at a distance $\simeq R^2/\lambda$. This depletion hole may play an important role in reflectivity experiments.[22]

To distinguish between a central regime with a characteristic lengths scale l and a distal regime with a characteristic length scale λ, these two length scales must be well separated. This is not always the case: In Figure 3 we show the solution of eq III.1 for nonvanishing values of $\tilde{\epsilon}$.

In the limit of infinite chain length, λ is always much larger than l. Nevertheless λ/l only increases as a power $^1/_6$ of the mass so that for finite masses the prefactors become important: They depend on both the bulk concentration and the adsorption strength. Upon decreasing the bulk concentrations, λ decreases and for weak bulk concentrations:

$$\phi_0 \ll \frac{a^2}{D^2}\exp\left[-1.5\left(\frac{N/D^2}{(\log(N/D^2))^2}\right)^{1/3}\right]$$

λ becomes much smaller than l and the tail concentration dominates only in the distal region. Note that for infinitely long chains, this requires a concentration exponentially weak in the molecular weight. This we call the *starved regime*. The tail contribution to U is dominated either by the loop contribution (close to the wall for $z < \lambda$) or by ϵ (further from the wall) and is

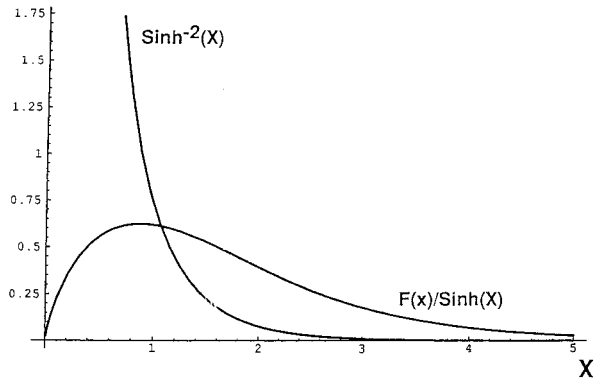

Figure 4. Plot of the reduced loop and tail contributions $\sinh^{-2}(X)$ and $F(X)/\sinh(X)$ in the starved regime.

thus negligible everywhere. In this regime the order parameter eq II.3 can be integrated analytically in a closed form. The loop contribution to the concentration ψ^2 is the same as in the usual ground state dominance approximation:

$$\psi = \frac{a}{\sqrt{3}\lambda \sinh(z/\lambda + b)} \qquad \text{(III.9)}$$

with $\coth(b) = \lambda/D$. Nevertheless the concentration far from the wall ($z > \lambda$) is dominated by the tail contribution, and its exponential decay length is 2 times that obtained from the usual ψ^2 given by eq III.9. The order parameter φ reads

$$\varphi = \frac{3\lambda^2}{a^2} F(z/\lambda + b)$$

$$F(X) = 1 - \frac{1}{\sinh(X)} \int_0^X \frac{X'}{\sinh(X')}\, dX' + (\cosh(X) - X/\sinh(X)) \log(\coth(X/2)) \qquad \text{(III.10)}$$

For simplicity the integration constants in $F(X)$ correspond to the case $b = 0$, and the finite value of b can be taken into account by a translation of the argument $X \rightarrow X + b$ with an accuracy $1/N$. Therefore the explicit loop and tail contributions to the concentration

$$c_l = \psi^2$$

$$c_t = \frac{2}{N} \frac{\coth b - 1}{\log \coth(b/2)} \frac{F(z/\lambda + b)}{\sinh(z/\lambda + b)} \qquad \text{(III.11)}$$

The reduced loop contribution $\sinh(X)^{-2}$ and tail contribution $F(X)/\sinh(X)$ are plotted in Figure 4. Many of the experimental results are expected to belong to the starved regime because $(N/\log(N)^2)^{1/3}$ is usually not a large number.

2. Semidilute Regime ($\phi_0 > 1/N$). The semidilute bulk solution is characterized by the correlation length of the concentration fluctuations,[23] in the mean-field approach:

$$\xi^2 = \frac{a^2}{3\phi_0} \qquad \text{(III.12)}$$

The bulk correlation length ξ becomes smaller than the concentration independent crossover length l, eq III.2 for concentrations larger than $\phi_1 \simeq (DN)^{-2/3}$. A detailed analysis of the order parameter eq II.3 shows that for $\phi_0 \gg \phi_1$, the distance z^* at which the loop and the tail contribution cross is increasing with concentration:

$$z^* \simeq N \phi_0 D \qquad \text{(III.13)}$$

Strictly speaking eq III.3 and the corresponding expression for z^* apply at a concentration defined by $\epsilon = \phi_0$ that is close to the overlap concentration. It is only approximate over the whole dilute regime. A more careful analysis shows that z^* is decreasing when the concentration is increasing from zero, as can be checked in the starved regime; z^* is thus predicted to go through a minimum.

At concentrations larger than $\phi_2 \simeq (D^2N)^{-1/2}$, the adsorption becomes weak in the sense that the bound state does not dominate the partition function of a chain with its end close to the wall ($N\epsilon \ll 1$). The above order parameter equations are only valid for distances much smaller than the chain radius R where the loops are dominant. The concentration profiles are obtained in two steps: We first determine the concentration profile for $N \rightarrow \infty$ and then calculate finite size corrections.

The standard ground state dominance approximation is valid for $z \ll R$:

$$\psi = \sqrt{\phi_0} \coth\left(\frac{z}{\xi} + b\right)$$

$$c_l = \psi^2 \qquad \text{(III.14)}$$

with $\sinh(2b) = 2D/\xi$. For $z \ll R$ the order parameter eq II.3 links φ to ψ, the latter being given by (III.14). In the crossover region ($z \simeq \xi$), 1 is negligible on the right-hand side of the equation for the order parameter φ. This gives

$$\varphi(z) = cst \int_D^z \frac{1}{\psi(z')^2}\, dz'$$

so that:

$$c_t = cst\, z \coth(z/\xi + b) \frac{f(z/\xi + b) - f(b)}{1 - f(b)}$$

$$f(x) = \coth(x) - 1/x$$

On the other hand, for large z, $z \gg R$, the potential U is localized in the adsorption layer and can be taken into account by a reflecting boundary condition at the wall:

$$c_l = 4\phi_0 i^2 erfc(z/R)$$

$$c_t = 8\phi_0 (i^2 erfc(z/2R) - i^2 erfc(z/R))$$

where $i^2 erfc(x)$ is a repeated integral of the error function defined in ref 24. Matching these results with those for short distances ($z \ll R$) gives the loop and tail contributions for all distances:

$$c_l = 4\phi_0 i^2 erfc(z/R) \coth^2\left(\frac{z}{\xi} + b\right)$$

$$c_t = (8\phi_0 (i^2 erfc(z/2R) - i^2 erfc(z/R))) \times \coth(z/\xi + b) \frac{f(z/\xi + b) - f(b)}{1 - f(b)} \qquad \text{(III.15)}$$

The study of the finite size corrections, done in ref 11, shows that the total concentration presents weak

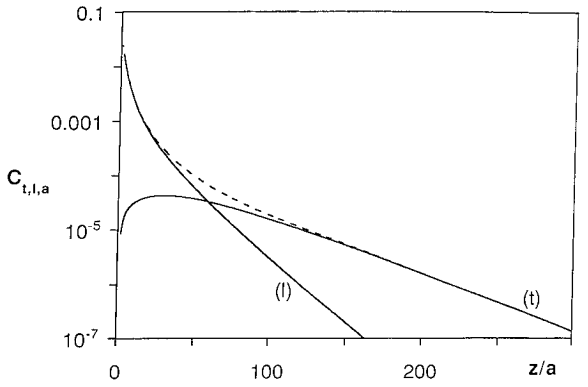

Figure 5. Loop and tail concentrations for $N = 100\,000$ and $\chi_s = 0.25$ from the numerical work. The loop contribution decays monotonically from the wall; the dashed line represents the total concentration built up by the adsorbed chains.

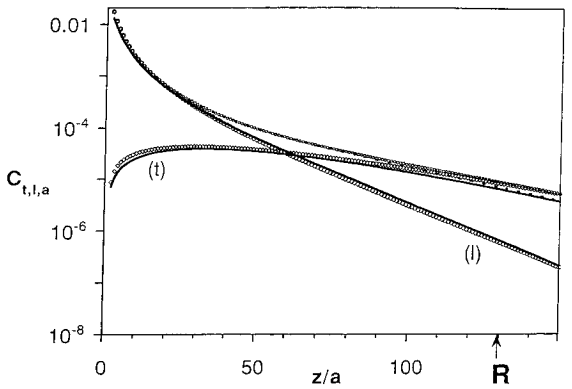

Figure 6. Fit of the numerical concentrations for $N = 100\,000$, $\chi_s = 0.25$, and $\phi_0 = 10^{-7}$ by the analytical results in the starved regime ($b = 0.1$).

oscillations. The first minimum is located at $z \simeq \xi \log(DR^4/\xi^5)$ and the first maximum at $z = 3.5R$.

More generally, a depletion hole is also predicted throughout the semidilute regime. The depletion effect is maximum for bulk concentrations slightly higher than the overlap concentration ($1/N < \phi_0 < \epsilon$). At higher concentrations the minimum is located around $z = \lambda$.

IV. Interpretation of the Numerical Mean-Field Results

The so-called Scheutjens and Fleer self-consistent mean-field theory leads to detailed numerical results for the loop and tail contributions to the adsorption profiles. We use here the results obtained by Van der Linden from the Scheutjens and Fleer method at bulk concentration $\phi_0 = 0.01$ and 10^{-7}, for chain lengths ranging from 500 to 100 000, and surface Flory parameters $\chi_s = 1$ or 0.25. These results are compared quantitatively with the analytical results (summarized in section III) in the various concentration regimes.

1. Starved Regime. The numerical results for $N = 100\,000$, $\phi_0 = 10^{-7}$, and $\chi_s = 0.25$ are presented in Figure 5. From the exponential decay at large distances, we obtain the size of the adsorbed layer $\lambda = 36a$, where a is the lattice constant. From eq III.7, we obtain $\epsilon = 14 \times 10^{-5}$. The tail contribution to the molecular potential U is never dominant; this corresponds to a starved adsorption.

The loop concentration can be fitted to eq III.11 with $\lambda = 36a$ and $b = 0.1$. This corresponds to $D = \lambda \tanh(b) = 3.6a$. The values of D, ϕ_0, N, and λ are then consistent with eq III.7.[25]

It is more difficult to relate the value of b to the value of χ_s in the Scheutjens and Fleer lattice theory. A naive transposition leads to $D \simeq a/[6(\chi_s - \chi_{s,c})]$. The Dutch group usually assumes that the adsorption threshold $\chi_{s,c}$ is given by the entropic contribution[26] $\chi_s = \log(6/5) = 0.18$. This would lead to the value $D \simeq 2.5a$. The concentration profiles closest to the wall depend upon the very detail of both the chain structure and the monomer/wall interaction. These are ignored by our continuous model that only applies for fairly dilute layers at distances from the wall larger than the actual monomer/wall interaction range.

The loop and tail concentrations for $N = 100\,000$, $\phi_0 = 10^{-7}$, and $b = 0.1$ computed from eq III.11, are plotted on Figure 6; the points are the numerical results from the Scheutjens and Fleer calculation. The analytical results are accurate for $z < R = 130a$, as expected.

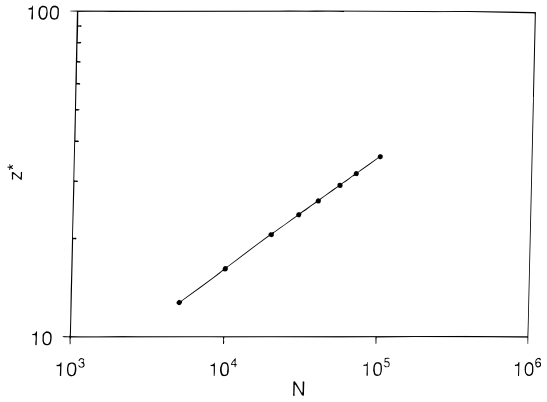

Figure 7. Plot of z^* versus N in log/log scale for fixed dilute bulk concentration ($\chi_s = 1$, $\phi_0 = 10^{-7}$). The slope is very close to $1/3$.

2. Dilute Regime. We now consider a set of numerical results for various chain lengths $N = 1000-100\,000$ with a strong adsorption enthalpy $\chi_s = 1$ and dilute bulk solutions $\phi_0 = 10^{-7}$. The cut-off length λ is, in this case, never much larger than l. We nevertheless expect z^* to be proportional to $N^{1/3}$. This is checked in the log/log plot displayed in Figure 7. The logarithmic factor of eqs III.2 and II.2 has a too weak variation to be observed here. The prefactor is however rather consistent; for the typical example below, the analytics give $z^* = 29a$ (where the factors D/a of only weak influence on the results have been discarded), whereas the numerics give the close value $z^* = 26a$.

A typical case is $N = 40\,000$, $\phi_0 = 10^{-7}$, and $\chi_s = 1$. From the Scheutjens and Fleer results, we find $z^* = 26a$, $\lambda = 23a$, and $z^*/\lambda = 1.13$. The reduced concentration profiles ($c_{t,l}z^{*2}$ versus z/z^*) corresponding to the same z^*/λ ratio obtained from eq III.1 are plotted on Figure 8 together with the numerical points. The agreement is good up to the radius of gyration R. The profiles are computed for $D = 0$. The finite adsorption strength should be accounted for by the proper boundary conditions or approximated by a shift of $z \rightarrow z + D$ along the z-axis. This only matters very close to the wall where the agreement is indeed worse.

All the numerical profiles show a depletion hole in the total concentration. The location z_{min} of the (shallow) minimum is plotted in Figure 9 for various chain lengths at fixed concentration ($\phi_0 = 10^{-7}$). As expected the location of the minimum z_{min} increases linearly with

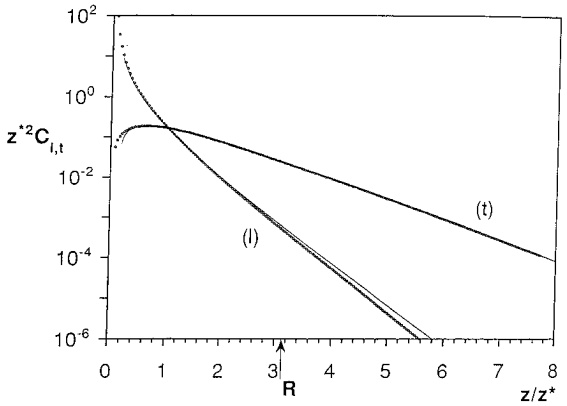

Figure 8. Fit of numerical results for $N = 40\,000$, $\chi_s = 1$, and $\phi_0 = 10^{-7}$ by the analytical laws in the dilute regime for $z^*/\lambda = 1.13$. The loop (l) and tail (t) contributions are represented, and data points correspond to the numerics. The loop contribution decays monotonically from the wall.

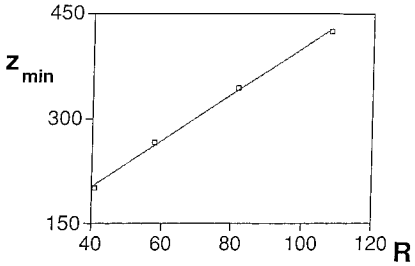

Figure 9. Depletion hole location in the dilute regime versus gyration radius.

the free chain radius $R \simeq R^2/\lambda$ at fixed bulk concentration. The limit $z_{min} \gg R$ is however not reached.

3. Semidilute Regime. For increasing bulk concentrations, z^* becomes concentration dependent as shown in Figure 10 from the Dutch group's results. Consistently with the analytical results, z^* goes through a minimum and increases linearly at higher concentrations before reaching a high concentration plateau. From the numerics, the location of the minimum seems to be proportional to $1/N$ (see Figure 10). The concentration regimes are not well separated in practice, and a more detailed comparison is uneasy.

We now consider strongly adsorbing, long chains $N = 40\,000$ and $\chi_s = 1$ in a rather concentrated solution of $\phi_0 = 0.01$. The numerical results show that the adsorbance is not dominated by the short loops, but the limit $\phi_0 \gg \phi_2$ is not reached. The analytical solution of eq III.15 is plotted together with the Scheutjens and Fleer results in Figure 11. The agreement is not quite as good. This is probably due to the fact that large loops and tails do not strongly dominate the adsorbance so that the bound state still has some importance.

In the numerical profiles, the depletion effect is never very pronounced. Nevertheless after a linear increase with ϵ at low ϵ, the depth of the depletion hole goes through a maximum at $\epsilon \simeq \phi_0$, as seen in Figure 12. The location z_{min} of the depletion hole increases linearly with λ as expected.

V. Beyond Mean Field

1. Extension of the Order Parameter Approach. It is appealing to extend the order parameter approach to obtain scaling laws for the polymer swollen in a good

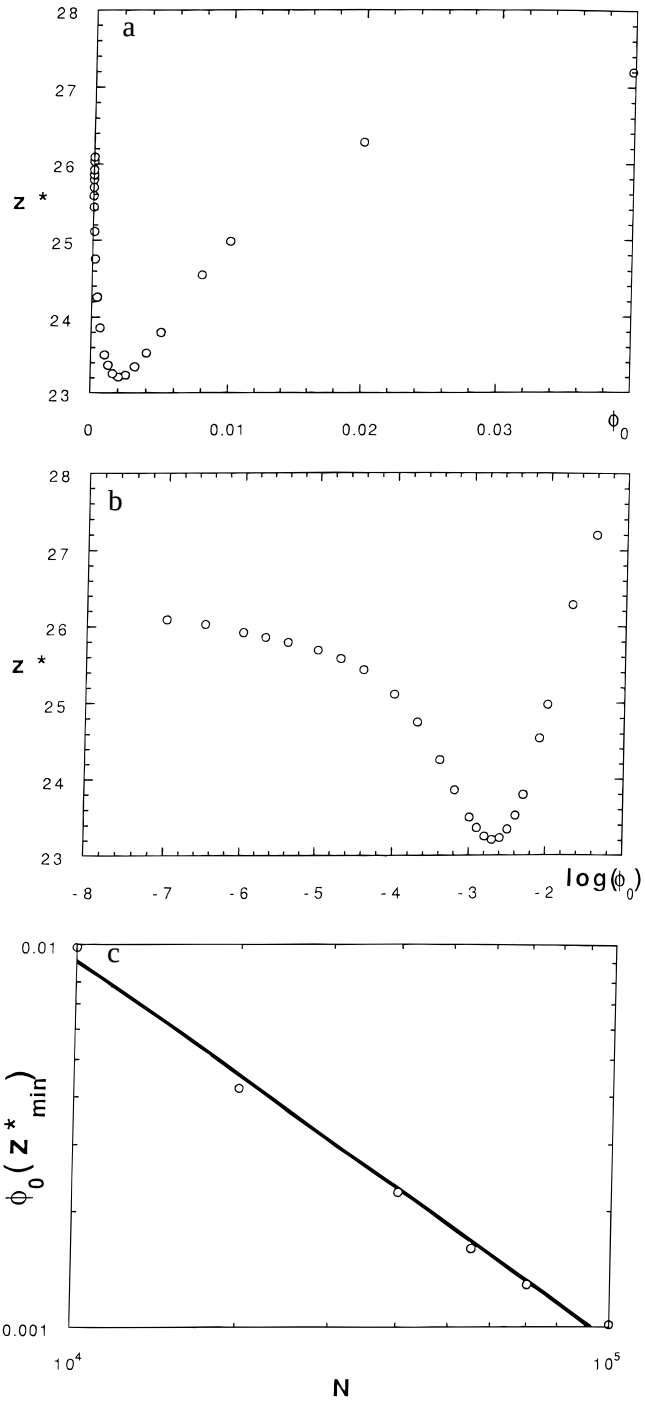

Figure 10. Length z^* at finite concentration: (a) crossover length z^* versus ϕ_0 plot (from the numerics for $N = 40\,000$), (b) crossover length z^* versus ϕ_0 semilogarithmic plot enhancing the dilute regime (from the numerics for $N = 40\,000$), and (c) location of the minimum in parts a and b, plotted against chain length (from the numerics).

solvent. We propose an oversimplified approach that preserves the structure of Edwards equation. In a semidilute bulk solution, the overall chain statistics are Gaussian, and one merely has to account for a local swelling of the chain at the scale of the correlation length. For weak concentration modulations, the energy of a chain configuration $\mathbf{r}(s)$ is evaluated as:[27,28]

$$L = \int_0^N \left[\phi^{1/4}\left(\frac{d\mathbf{r}}{ds}\right)^2 + U\right] ds \qquad (V.1)$$

where the potential U is linked to the local concentration

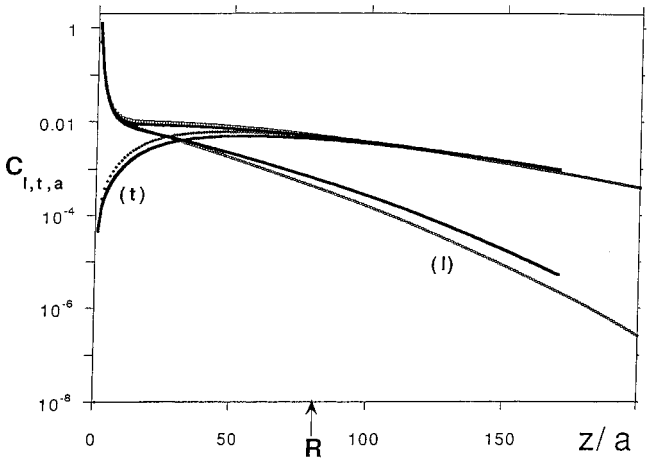

Figure 11. Fit of the numerical work for $N = 40\,000$, $\chi_s = 1$, and $\phi_0 = 10^{-2}$, by the analytical results for $\phi_0 > \phi_2$. The loop (l) concentration (decaying from the wall), the tail concentration (t), and the total concentration of adsorbed polymer are represented. Data points correspond to the numerical work.

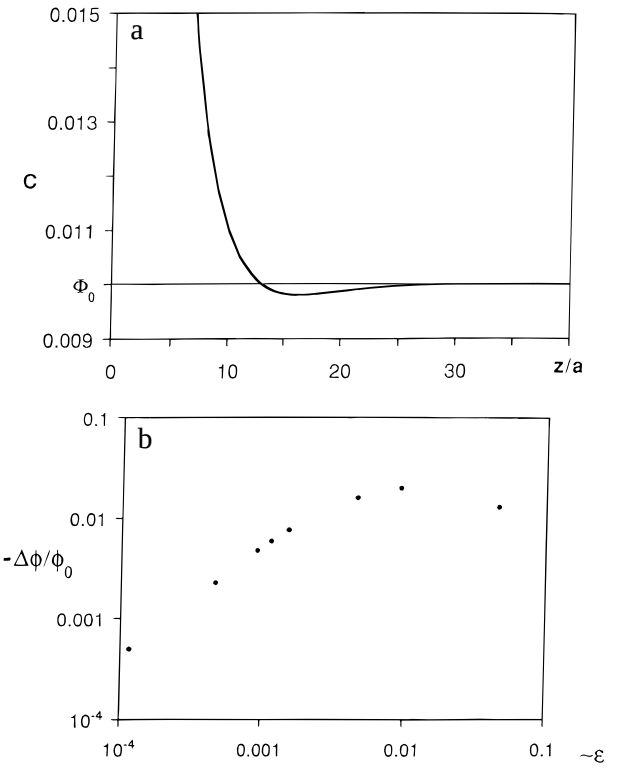

Figure 12. Depletion hole at finite concentration ($\phi_0 = 0.01$): (a) total concentration profile ($N = 500$, $\chi_s = 1$, $\phi_0 = 0.01$) showing the depletion hole and (b) relative depth of the depletion hole versus $1/N$ log $1/\phi_0$. The latter is of order ϵ around the maximum.

ϕ through

$$U = C\phi^{5/4}$$

with C a constant (or order unity) that can be determined from the structure factor of a semidilute solution.[29-31] Strictly speaking eq V.1 assumes weak concentration modulations at the scale of the local correlation length. These are rather of order 1 in the strong adsorption limit where the results can thus not be expected to be very accurate. The first term in eq V.1 has the standard Gaussian form after the change of coordinates,[27] $d\mathbf{R} = \phi^{1/8}\, d\mathbf{r}$. The prescribed L does not couple the space directions. For the adsorption problem, it is enough to consider the coordinate z normal to the wall:

$$L = \int_0^N \left[\left(\frac{dZ}{ds}\right)^2 + U\right] ds \qquad \text{(V.2)}$$

The chain propagator follows then Edwards equation:

$$-\frac{\partial G}{\partial s} = -\frac{a^2}{6}\frac{\partial^2 G}{\partial Z^2} + C\phi^{5/4}G \qquad \text{(V.3)}$$

It is then possible to repeat the mean-field calculation of section III. The order parameter equations then read eq II.3:

$$0 = -\frac{a^2}{6}\frac{\partial^2 \psi}{\partial Z^2} + (C(\phi^{5/4} - \phi_0^{5/4}) + \epsilon)\psi$$

$$1 = -\frac{a^2}{6}\frac{\partial^2 \varphi}{\partial Z^2} + (C(\phi^{5/4} - \phi_0^{5/4}) + \epsilon)\varphi \qquad \text{(V.4)}$$

where the local concentration ϕ is linked to the order parameters through

$$\phi = N\left(\psi\psi + \frac{2}{N}\psi\psi\right)\frac{dZ}{dz}$$

with N a normalization constant relating the concentration and the statistical weight of the configurations.

Here, we only describe the central regime in the dilute case to illustrate the method. As in section III, the order parameter equations can be written in reduced form (eq III.1). This introduces the natural units:

$$L^2 = \frac{a^2}{6}C^{-7/27}N^{-10/27}(N/2)^{20/27}$$

$$\varphi^* = 6L^2/a^2 \qquad \text{(V.5)}$$

$$\psi^* = 12L^2/Na^2$$

Close to the wall ($z < l$), the concentration is dominated by the loops and

$$U = A_I Z^{-2}$$

with

$$A_I = \frac{a^2}{6}\frac{119}{100}$$

$$c_l = \frac{U^{4/5}}{C} \simeq z^{-4/3} \qquad \text{(V.6)}$$

$$c_e = \frac{2}{N}N^{1/2}A_I^{4/5}Z^{-9/10} \simeq z^{-3/4}$$

$$c_t \simeq \frac{1}{N}z^{2/3}$$

Further away from the wall ($z > l$), the concentration

is dominated by the tails and

$$U = A_{II} Z^{-2}$$

with

$$A_{II} = \frac{a^2}{6}\frac{374}{25}$$

$$c_l \simeq z^{-35/6} \tag{V.7}$$

$$c_e = \frac{1}{K}\left(\frac{A_{II}}{C}\right)^{4/5} Z^{-18/5} \simeq z^{-3}$$

with

$$K = A_{II} - a^2/3$$

$$c_t \simeq z^{-4/3}$$

From the asymptotics we determine the normalization constant N ($N \simeq N^{-1/4}$), wherefrom:

$$l \simeq N^{1/2}$$

Finally the prefactor of the $z^{-4/3}$ power law is found to be larger by a factor of 5.4 when $z > l$ than when $z < l$.

2. Scaling Results. We have constructed scaling laws for the partition functions and therefore for the relevant concentrations in all bulk concentration regimes.[11] Here we only recall the results for the central regime in order to compare with those of previous subsection V.1. Close to the wall ($z < l \simeq N^{1/(d-1)}$):

$$c_l \simeq z^{1/\nu - d}$$

$$c_e \simeq \frac{1}{Nl}\left(\frac{z}{l}\right)^{-\beta/\nu} \tag{V.8}$$

$$c_t \simeq \frac{1}{N} z^{1/\nu - 1}$$

whereas for $z > l \simeq N^{1/(d-1)}$,

$$c_l \simeq N^{(\gamma+\nu d)/\nu(d-1)} z^{(-2\nu d+1-\gamma/\nu)}$$

$$c_e \simeq \frac{1}{z^d} \tag{V.9}$$

$$c_t \simeq z^{1/\nu - d}$$

These scaling laws agree with the mean-field asymptotics eqs III.4 and III.5 for $\nu = {}^1/_2$, $d = 4$, and $\gamma = 1$, as they should.

A comparison between eqs V.6 and V.7 and eqs V.8 and V.9 shows that the proposed extension of the order parameter approach gives exponents close or equal to the excluded volume exponents. In fact eq V.1 is constructed with the only exponent ν (approximated by the Flory value ${}^3/_5$). The resulting theory properly accounts for ν and d in the various exponents but consistently replaces the susceptibility exponent γ close to 1.16 by the unphysical value 0.9. This merely affects the end distribution close to the wall. Although we are aware of its weaknesses, we expect that this approach leads to improved numerical prefactors (*e.g.*, the amplitude ratio A_{II}/A_I) with respect to mean field.

VI. Conclusion

In a recent paper we have studied theoretically the adsorption of a neutral homopolymer onto a flat surface within the framework of a mean-field model with two order parameters. In the present paper we present an explicit comparison between numerical mean-field results from the so-called Scheutjens and Fleer theory and the analytical mean-field results obtained from the order parameter approach. We show that the numerical results of the Scheutjens and Fleer calculation, which have been known now for some time,[3,10,9] can be quantitatively explained by the mean-field theory with two order parameters.[11] Furthermore, both previous scaling arguments[11,15] and an extension of the analytical theory show that a similar picture holds qualitatively for self-avoiding polymer chains. The analytical theory introduces five length scales: D, ξ, z^*, λ, and R. D is the so-called adsorption length and depends only on the adsorption strength. ξ is the bulk correlation length (only defined for semidilute bulk solutions). z^* is the distance from the wall where tail monomers start to dominate over loop monomers. λ is the thickness of the adsorbed polymer layer. R is the radius of gyration of the polymer chain. For infinitely long chains, several regimes can be defined depending on the relative magnitude of these length scales. The numerical results have been obtained over a wide range of parameters.

We have checked the dependence of the characteristic length scales on the relevant parameters (N, ϕ_0). The numerical loop and tail contributions show a good agreement with the analytical results. The location and depth of the depletion hole in the total concentration (including free chains) also compare well with the theoretical predictions. In all cases the agreement is good, and the analytical approach explains the numerical data. Nevertheless, the true asymptotic regime of infinitely long chains is never reached in the numerical work (and maybe in experiments). As an example, the adsorbance Γ is predicted to go through a maximum as a function of chain length and to decrease for very long chains.[11] This decrease is not observed in the numerical data. Many numerical data are obtained for moderately long chains ($N \simeq 1000$) and rather correspond to starved adsorption.

In the order parameter theory, the free energy density is approximated by the second virial expansion; it is inaccurate for densities close to that of the melt as encountered at the wall in cases of very strong adsorption where the relevance of equilibrium theory is questionable anyhow. In the continuous theory the interaction between a monomer and the wall is only taken into account by a boundary condition, and it is valid at distances much larger than the actual wall/monomer potential width; this makes detailed comparison with the numerical lattice theory difficult closest to the wall.

We also have proposed a simplified extension of the order parameter theory to account for excluded volume statistics. This theory allows to determine explicit concentration profiles. A comparison of the obtained asymptotic behaviors with the known scaling laws[15,11] shows that the exponents are rather accurate or even exact. Only the exponents depending upon the susceptibility exponent γ close to 1.16 (not entering the (oversimplified) extended order parameter theory) are

not exact, and γ is systematically replaced by the unphysical value 0.9.

At this point, numerical simulations of adsorbing chains swollen in a good solvent would be of major interest. As far as we are aware of, there are no numerical results published on the adsorption of self-avoiding chains at finite concentration, but simulations by Sommer are in progress.[32]

Acknowledgment. We thank G. Fleer and M. Cohen Stuart for discussions on their results. This work was performed during the stay of one of the authors (A.N.S.) at Université Louis Pasteur in Strasbourg (Institut Charles Sadron). A.N.S. would like to thank the university and the Ministry of Higher Education of France for the opportunity to stay in Strasbourg.

References and Notes

(1) Auroy, P.; Auvray, L.; Leger, L. *Macromolecules* **1991**, *24*, 5158.
(2) Napper, D. H. *Polymeric Stabilization of Colloidal Dispersions*; Academic Press: London, 1983.
(3) Fleer, G. J.; Cohen Stuart, M. A.; Scheutjens, J. M. H. M.; Cosgrove, B.; Vincent, B. *Polymers at Interfaces*; Chapman and Hall: London, 1993.
(4) Ajdari, A.; Brochard-Wyart, F.; de Gennes, P. G.; Leibler, L.; Viovy, J. L.; Rubinstein, M. *Physica A* **1994**, *204*, 17.
(5) Raphael, E.; de Gennes, P. G. *J. Phys. Chem.* **1992**, *96*, 4002.
(6) Senden, T.; di Meglio, J. M.; Auroy, P. Preprint, 1995.
(7) Maaloum, M. Preprint, 1995.
(8) Silberberg, A. *J. Phys. Chem.* **1962**, *66*, 1972; **1962**, *66*, 1884.
(9) Ploehn, H.; Russell, W. B. *Macromolecules* **1989**, *22*, 266.
(10) Scheutjens, J.; Fleer, G. *J. Phys. Chem.* **1980**, *84*, 178.
(11) Semenov, A. N.; Bonet Avalos, J.; Johner, A.; Joanny, J. F. *Macromolecules*, in press.
(12) de Gennes, P. G. *Adv. Coll. Interf. Sci.* **1987**, *27*, 189.
(13) de Gennes, P. G. *Phys. Lett.* **1972**, *A38*, 339.
(14) Eisenriegler, E. *Polymers near Interfaces*; World Scientific Publishing: Singapore, 1993.
(15) Semenov, A. N.; Joanny, J. F. *Europhys. Lett.* **1995**, *29*, 279.
(16) Marques, C. M.; Joanny, J. F. *J. Phys. (France)* **1988**, *49*, 1103.
(17) Daoud, M.; Jannink, G. *J. Phys. (France) I* **1991**, *1*, 1493.
(18) Guiselin, O. Thesis, Paris, 1992.
(19) Guiselin, O. *Europhys. Lett.* **1992**, *17*, 225.
(20) Eisenriegler, E.; Kremer, K.; Binder, K. *J. Chem. Phys.* **1982**, *77*, 6297.
(21) Edwards, S. F. *Proc. Phys. Soc.* **1965**, *85*, 613.
(22) Lee, L. T.; Guiselin, O.; Farnoux, B.; Lapp, A. *Macromolecules* **1991**, *24*, 2518.
(23) de Gennes, P. G. *Scaling Concepts in Polymer Physics*; Cornell: Ithaca, NY, 1985.
(24) Abramowitz, M.; Stegun, I. *Handbook of Mathematical Functions*; Dover: New York, 1972.
(25) The length D can also be estimated by identifying the discrete lattice equations with the continuous equations in the first layer; the value $D/a = 3.72$ is then found (G. Fleer, Wageningen, The Netherlands, private communication).
(26) van der Linden, C.; Leermakers, F. *Macromolecules* **1992**, *25*, 3449.
(27) Milner, S.; Witten, T.; Cates, M. E. *Macromolecules* **1988**, *21*, 2610.
(28) Johner, A.; Joanny, J. F.; Rubinstein, M. *Europhys. Lett.* **1993**, *22*, 591.
(29) de Gennes, P. G. *Macromolecules* **1981**, *14*, 1637; **1982**, *15*, 500.
(30) des Cloizeaux, J.; Jannink, G. *Les Polymeres en Solution*; Les Ulis: France, 1987; Editions de Physique.
(31) Brooks, J.; Cates, M. E. *Macromolecules* **1992**, *25*, 391.
(32) Sommer, J. U. Private communication.

MA951637J